The object of this study is a new design of an overhead microstrip antenna, including Epsilon Negative (ENG) metamaterials and L-shaped parasitic overlays aimed at achieving dual-band operation and improving the performance of modern wireless communication systems. The research is aimed at solving the problem of limited bandwidth and dual-band functionality in conventional antenna designs.

This study solves the problem of limited bandwidth and dual-band functionality in conventional microstrip patch antenna designs, which are crucial for modern wireless communication systems. The inclusion of L-shaped parasitic overlays effectively expands the bandwidth in each frequency range.

The results indicate significant improvements: at the upper resonant frequency, a 10 dB return loss bandwidth of 27.84 % (2.88–3.81 GHz) and a 3 dB axial ratio bandwidth of 5.05 % (2.90–3.05 GHz) are achieved, while at the lower resonant frequency, a return loss bandwidth is 10 dB, which is 6.11 % (2.22–2.36 GHz). These improvements indicate a significant increase in antenna performance compared to conventional designs, which is confirmed by comparing the simulation results with the measurement results.

Distinctive features contributing to these results include the use of ENG metamaterials, which improve electromagnetic properties and signal propagation; vertical transitions, which provide efficient dual-band operation; and L-shaped parasitic overlays, which significantly expand bandwidth. These characteristics combine to eliminate the limitations of traditional designs, which makes the proposed antenna suitable for use in a wide frequency range in modern wireless communication systems

Keywords: Minkowski fractal, epsilon negative metamaterials, parasitic patches, dual-band, health care system

DEVELOPMENT OF AN INNOVATIVE PATCH ANTENNA DESIGN AND IMPLEMENTATION USING ENG MATERIALS FOR HEALTH CARE SYSTEMS AND 5G NETWORKS

Nagima Bakirova
Senior Lector, PhD Doctoral Student
Academy of Logistics and Transport*

Pramod Kumar
Professor
Department of Electrical Communication Engineering
B. V. Raju Institute of Technology
Vishnupur, Narsapur, Taljarampet, Telangana, India, 502313

Suman Nelaturi
PhD, Associate Professor
Department of Electrical Communication Engineering
Vignan's Foundation for Science, Technology and Research
Guntur-Tenali Rd, Vadlamudi, Andhra Pradesh, India, 522213

Tansaule Serikov
Doctor PhD**

Marzhan Temirbekova
PhD, Associate Professor***

Gani Sergazin
PhD, Associate Professor***

Gulzada Mussapirova
Assistant Professor
Department of Information Communication Technologies*

Arai Tolegenova
PhD, Associate Professor**

Akmaral Tlenshiyeva
Senior Lector
Department of Information and Communication Technologies***

Ruslan Kassym
Corresponding author
Supervisor Project
Department of Information and Communication Technologies***
E-mail: kasym.ruslan@gmail.com
*Gumarbek Daukeyev Almaty University of Power Engineering and Telecommunications
Baytursynuli str., 126/1, Almaty, Republic of Kazakhstan, 050013
**Department of Information Communication Technologies
S. Seifullin Kazakh Agrotechnical Research University
Zhenis ave., 62, Astana, Republic of Kazakhstan, 010011
***ALT University
Shevchenko str., 97, Almaty, Republic of Kazakhstan, 050013

1. Introduction

The rapid evolution of wireless communication technologies such as WLAN, Wi-Fi, and Wi-MAX has led to an increasing demand for efficient and compact antennas. Microstrip patch antennas (MPAs) are a prime candidate due to their low profile, ease of fabrication, and versatility in multifunctional applications. Circularly polarized (CP)

antennas, in particular, are crucial for these applications as they help mitigate mismatches between receivers and transmitters, thus ensuring reliable communication.

Metamaterials, which possess unique artificial electromagnetic properties, offer a promising avenue for the advancement of miniaturized multiband antennas. The ability to engineer these properties opens up new possibilities for antenna design that are not achievable with conventional materials. This includes the development of epsilon negative transmission line (ENGTL) materials, permeability negative transmission line (MNGTL) materials, and composite right/left-handed (CRLH) transmission lines, each contributing differently to enhancing antenna performance. Research has shown that metamaterials can significantly improve the performance of antennas. For instance, the use of CRLH transmission lines can enable dual-band functionality and miniaturization, while epsilon negative materials can enhance bandwidth and signal propagation. Despite these advancements, there remain unresolved issues such as narrow bandwidth at each resonance frequency and complex fabrication processes, which hinder the practical application of these materials in commercial antenna designs.

Furthermore, with the proliferation of devices requiring high-speed wireless communication, there is an ongoing need for antennas that not only operate efficiently at multiple frequency bands but also maintain good impedance matching and minimize interference. Advances in fractal antenna designs and the incorporation of parasitic elements like vertical interconnect accesses (VIAs) and L-shaped patches have shown promise in addressing these challenges by enhancing bandwidth and polarization characteristics. Given the continuous expansion of wireless technologies and the demand for more efficient and compact antennas, research in this area remains highly relevant. The development of advanced antenna designs using metamaterials is critical to meeting the needs of modern communication systems, which require higher data rates, better connectivity, and more reliable performance.

Therefore, research on the development and optimization of metamaterial-based microstrip patch antennas is highly relevant. This ongoing exploration is essential to address the existing limitations and push the boundaries of current wireless communication technologies.

2. Literature review and problem statement

The work [1] presented a fractal-based MIMO antenna design for sub-6 GHz 5G applications, demonstrating the benefits of fractal geometry in enhancing bandwidth and reducing antenna size. However, the integration of these designs into even more compact 5G devices, particularly those used in constrained environments, remains a critical challenge. Similarly, in [2], the development of a fractal monopole MIMO antenna for modern 5G applications showed improvements in broadband performance and miniaturization. Despite these advancements, further research is necessary to optimize these designs for seamless integration into small healthcare devices without compromising performance. The paper [3] introduced a trident-shaped dual-band MIMO antenna with a novel ground plane, significantly enhancing bandwidth and isolation. Nonetheless, ensuring consistent performance in diverse operating environments and maintaining compact form factors continues to be problematic. The work [4] on a compact dual-band dual-mode circular patch antenna emphasized the importance of dual-mode operation. However, achieving a balance between unidirectional linear polarization and omnidirectional circular polarization in a compact and efficient design still presents a considerable challenge. The paper [5] developed a compact asymmetric microstrip antenna with circular polarization and fractal boundaries, highlighting the benefits of circular polarization in improving signal stability and reducing multipath interference. Yet, the challenge of achieving these benefits in devices used for reliable medical monitoring remains unresolved.

The work [6] on a three-band microstrip antenna with a fractal Koch boundary demonstrated improved performance across multiple frequency bands. Despite this, the consistent performance of these antennas in varying environmental conditions and applications, such as health monitoring and 5G communications, still requires further exploration. Finally, the paper [7] investigated a low-profile T-shaped, electrically small-sized antenna with metamaterial engraving for WLAN and 5G applications, showcasing the potential of metamaterials in creating compact and efficient antennas. However, the practical implementation and scalability of such designs in real-world applications continue to pose significant challenges.

The problem with the study is that existing antenna designs for 5G applications suffer from limited bandwidth and insufficient functionality in two frequency bands. Traditional antennas are difficult to integrate into compact devices such as medical devices without loss of performance. Stable operation of antennas in various operating conditions, as well as achieving a balance between different polarization requirements, remain serious challenges. In addition, the practical implementation and scalability of modern antennas for real-world applications face significant difficulties.

3. The aim and objectives of the study

The aim of the study is to develop a novel microstrip patch antenna (MPA) that incorporates epsilon negative (ENG) metamaterials and L-shaped parasitic patches to achieve dual-band operation and enhanced performance for modern wireless communication applications.

To achieve this aim, the following objectives are accomplished:

– to design and fabricate a microstrip patch antenna with integrated ENG metamaterials and L-shaped parasitic patches;

– to analyze the dual-band behavior and circular polarization characteristics of the antenna through simulations;

– to optimize the antenna design for improved bandwidth and polarization performance through iterative testing and refinement.

4. Materials and methods

The object of this study is to design a dual-band patch antenna with circular polarization at the upper frequency band and left-handed frequency at the lower resonating band. The main hypothesis of the study is that incorporating fractal geometry and shunt inductance via vertical VIAs can enhance the antenna performance. Assumptions made in the study include ideal material properties for the substrate and perfect electrical conductor behavior for the patches. Simplifications include ignoring the effects of environmental factors such as temperature and humidity.

The proposed design is developed using theoretical methods, involving electromagnetic field theory and antenna design principles. The antenna design is based on a dielectric constant of 2.2, with a thickness of 3.2 mm, using Rogers RT/Duroid 5880 substrate material. The antenna layout includes a main patch with four L-shaped parasitic patches printed on the top of the substrate and a square ground plane with four rectangular protrusions printed on the bottom. Four vertical VIAs, with a radius of 0.3 mm and height of 3.2 mm, are strategically placed to provide the necessary shunt inductance for achieving dual-band operation.

Theoretical simulations are conducted using electromagnetic simulation software to validate the proposed design. The software used for these simulations includes HFSS (High-Frequency Structure Simulator) and CST Microwave Studio, which are known for their accuracy in modeling and analyzing the electromagnetic behavior of antenna structures.

During the research, a dual-band patch antenna was developed using fractal Minkowski curves to achieve circular polarization in the upper frequency range. The depth of the fractal geometry is 0.4 mm on the x axis and 0.2 mm on the y axis, which ensures a stable axial ratio below 3 dB, providing effective circular polarization.

For the low frequency range, the left frequency response was achieved due to the strategic placement of vertical junctions with junctions providing the necessary shunt inductance to improve impedance matching. The transition holes were located at a distance of 7 mm from the center, which significantly expanded the bandwidth and stabilized the low-frequency response.

5. Results of the study of Minkowski fractal antennas

5. 1. Design and fabrication of a microstrip patch antenna with integrated ENG metamaterials and L-shaped parasitic patches

The design of the suggested patch antenna is depicted in Fig. 1, which shows the general appearance, top view, and bottom view of the antenna. The layout measurements of the suggested antenna are summarized in Table 1. These figures and tables provide a visual and quantitative representation of the antenna design parameters critical for the simulation and analysis process.

IF and IO are important parameters to consider when working with fractal curves. IF refers to indentation depth in a Minkowski fractal curve. The fractal patch antenna has Dx and Dy. They are the indentation depths laterally the x- and y-axes, respectively. The four parts of the square patch antenna are replaced with Minkowski fractal curve with an indentation depth of 0.4 along the x-axis and 0.2 along the y-axis to get circular polarization at the upper frequency band. Four vertical VIAs with a radius of 0.3 mm and height of 3.2 mm are placed across the circumference of the fractal patch to get lower resonating frequency band, which is also known as left handed frequency. The optimized location of VIAs is 7 mm from the center of the patch. It is proposed to position the optimal coaxial probe feed point along the diagonal.
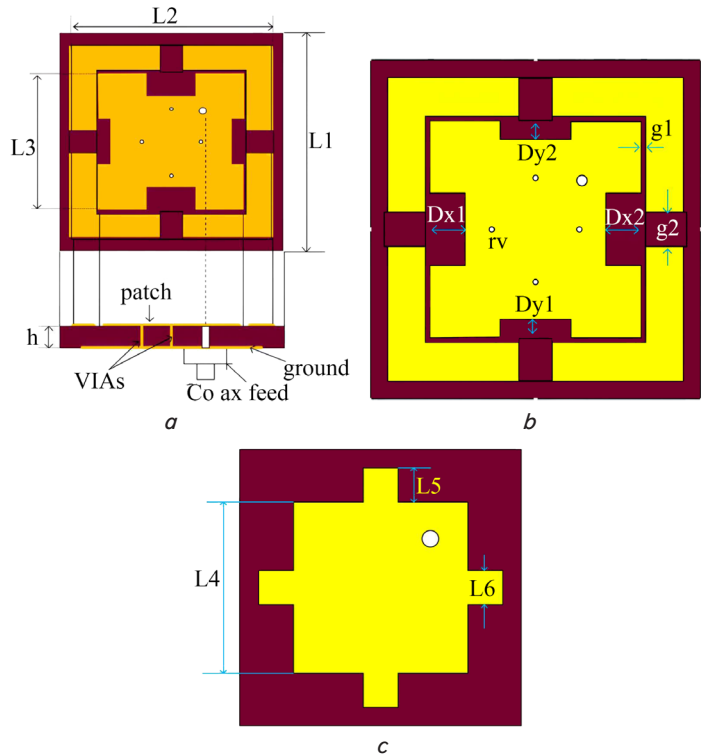

Fig. 1. The design of the recommended antenna and dimensions: a — general appearance; b — top rating; c — bottom rating

Table 1

Parameter values of Ant8

Parameter	Value in mm
$L1$	46
$L2$	42
$L3$	30
$L4$	36
$L5$	5.8
$L6$	4
$g1$	0.4
$g2$	4
Rv	0.3
H	3.175
$Dx1=Dx2$	4
$Dy1=Dy2$	1

5. 2. Analysis of dual-band behavior and circular polarization characteristics through simulations

Simulations were conducted to analyze the S-parameter features of the proposed antenna designs. The dual-band operation was achieved through the integration of vertical VIAs. The addition of parasitic elements increased the transmission capacity at each resonating frequency. Circular polarization was obtained using Minkowski fractal curves. The resonating frequencies and S_{11} loss bandwidths for each antenna iteration were documented, showing significant improvements in performance.

By examining and evolution of the suggested design patch antenna operation principles in the given Fig. 2. First, we selected a square patch antenna 1, it operates at a frequency of 3.05 GHz and produces linear polarization. All patch

antennas are depicted in Fig. 2. To accomplish the circular divergence here we introduced Minkowski fractal edges along the corners of the square patch, i.e. design 2 (Ant2). In Ant3, four L-shaped parasitic patches are proposed along the circumference of the square patch for increased linear polarization bandwidth. Ant4 represents the CP design version obtained by offering Minkowski fractal edges to the corners of Ant3. Ant5 to Ant8 are similar to Ant1 to Ant4, whereas the vertical VIAs are inserted to get lower resonating frequency (to obtain dual-band operation). Ultimately, Ant8 is the recommended antenna that produces dual band and dual polarization.
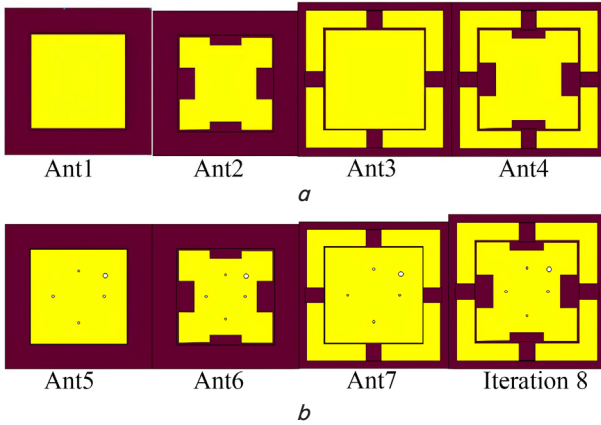
Fig. 2. Detailed structure of the proposed patch antennas: *a* — with a basic square overlay; *b* — with dual polarization

The antenna design evolved from a basic square patch (Ant1) to a dual-band, dual-polarized antenna (Ant8) by incorporating Minkowski fractal edges, L-shaped parasitic patches, and vertical VIAs. Each modification aimed to enhance bandwidth and polarization. The final design, Ant8, achieved dual-band operation with significantly improved S_{11} loss bandwidth, making it suitable for modern wireless communication applications.

5. 3. Optimization of antenna design for improved bandwidth and polarization performance

The final antenna design, Ant8, underwent optimization to improve its bandwidth and polarization characteristics. Indentation depths along the x- and y-axes were varied to alter the radiation characteristics. The optimized antenna showed a substantial improvement in S_{11} loss bandwidth, achieving 27.84 % at the upper frequency band and 6.11 % at the lower frequency band. The surface current distributions at 2.28 GHz and 3.15 GHz were analyzed using HFSS Simulation Software, demonstrating strong current distribution at VIAs and Minkowski fractal curves. The simulated and experimental results showed close correspondence, validating the effectiveness of the design.

The S-parameter features are simulated for all the suggested antennas and represented in Fig. 3. The dual-band operation is achieved by storing VIAs. The widened transmission capacity at each resonating frequency is obtained by loading parasitic elements. By using Minkowski fractal curves, we can obtain the circular polarization. The resonating frequencies of S_{11} loss bandwidth are recorded in Table 2.

Indentation Depths (ID) along the x- and y-axes are used to alter the radiation characteristics of patch antennas. The antennas are given in Fig. 4 and used to show variation in IDs.
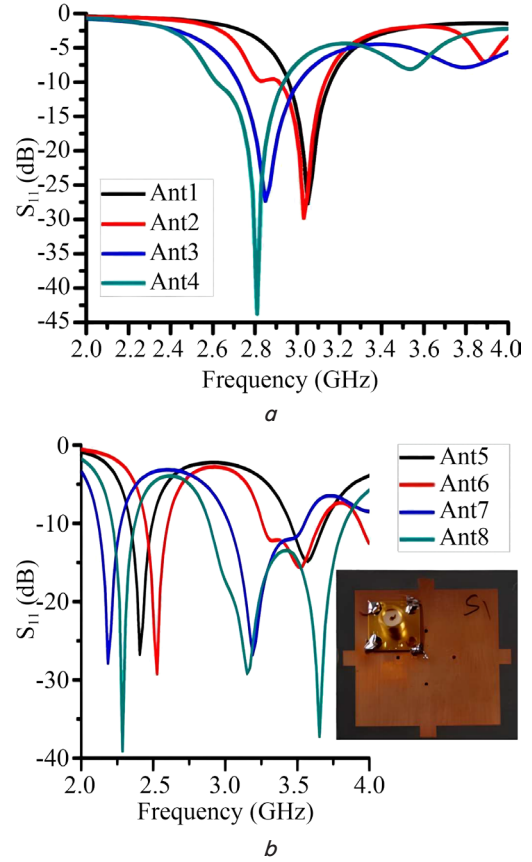

Fig. 3. Simulated S-parameter features: *a* — Ant1—Ant4; *b* — Ant5—Ant8

Table 2

Comparison table for simulation results of the proposed antenna

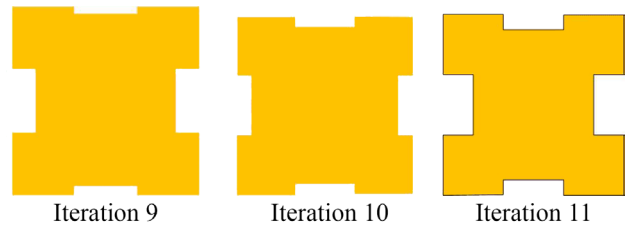| Ant	S_{11} loss bandwidth	
	at lower frequency	at upper frequency
Ant1	–	(2.96–3.15 GHz) 6.22 %
Ant2	–	(2.92–3.13 GHz) 6.95 %
Ant3	–	(2.72–2.98 GHz) 9.12 %
Ant4	–	(2.62–2.92 GHz) 10.83 %
Ant5	(2.34–2.48 GHz) 5.8 %	(3.47–3.67 GHz) 5.60 %
Ant6	(2.46–2.58 GHz) 4.76 %	(3.27–3.65 GHz) 10.98 %
Ant7	(2.12–2.26 GHz) 6.39 %	(3.03–3.53 GHz) 15.24 %
Ant8	(2.22–2.36 GHz) 6.11 %	(2.88–3.81 GHz) 27.84 %

Fig. 4. Dual-band dual-polarized antennas with different indentation depths

The dual-band dual-polarized antenna simulated return loss characteristics are observed with variation of IDs (Indentation Depths) and given in Fig. 5. The two operating bands impedance bandwidths are stated in Table 3.
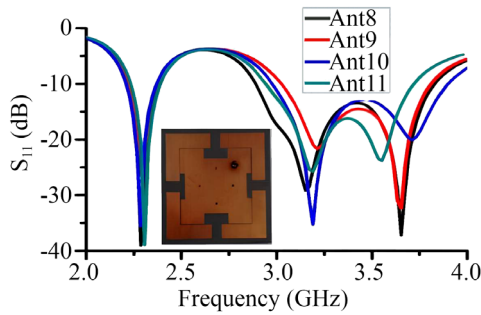
Fig. 5. The proposed antenna S_{11} characteristics with respect to variation of indentation depth

Table 3

Comparison of antennas with variation of indentation depth

Ant	ID (mm)		S_{11} loss bandwidth	
	Dx	Dy	at low frequency	at high frequency
Ant8 proposed	0.4	0.1	(2.22–2.36 GHz) 6.11 %	(2.88–3.81 GHz) 27.84 %
Ant9	0.3	0.1	(2.24–2.38 GHz) 6.06 %	(3.03–3.79 GHz) 22.2 %
Ant10	0.3	0.2	(2.22–2.36 GHz) 6.11 %	(2.96–3.87 GHz) 26.6 %
Ant11	0.4	0.2	(2.24–2.38 GHz) 6.06 %	(2.94–3.71 GHz) 23.19 %

The surface current distribution of Ant8 is represented in Fig. 6 at respective frequencies of 2.28 GHz and 3.15 GHz. This is done with the help of HFSS Simulation Software. From Fig. 6 we know the operational mechanism of the suggested antenna.
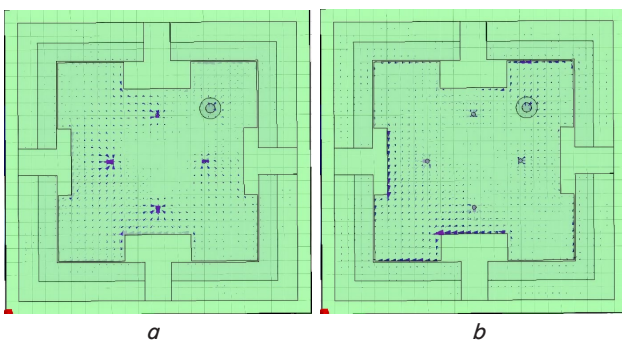

Fig. 6. Proposed antenna current distribution:
a — at 2.28 GHz; b — at 3.15 GHz

At VIAs, the lower resonating frequency (2.28 GHz) surface current distribution is strong. Similarly, at Minkowski fractal curves of the patch the upper resonating frequency (3.15 GHz) becomes strong.

The developed Ant8 is illustrated in Fig. 7. The vertical metallic VIAs are inserted in the patch by using through hole copper plating technique. RLC was measured using an Agilent 8719A microwave network analyzer. Similarly, the radiation pattern characteristics are measured with the aid of anechoic chamber; it has

physical dimensions of $22.5 \times 12.5 \times 11.5$ m³. The anechoic chamber is operated at 400 MHz to 18 GHz.

The simulation and experimental RLC results are displayed in Fig. 8. The empirical and simulation outcomes are in close synchronization (or harmony). The possibility of circular polarization is due to the discontinuity at the upper resonating band. At high and low operating frequency bands, the return loss bandwidths are 27.84 % (2.88–3.81 GHz) and 6.11 % (2.22 GHz–2.36 GHz) due to current at VIAs, respectively. The simulation and experimental characteristics of the axial ratio are presented in Fig. 8, b. At higher resonating frequency, the measured 3-dB axial ratio bandwidth is 5.05 % (2.90 GHz–3.05 GHz). Similarly, at the center frequency we obtained the minimum axial ratio value of 0.3 dB.
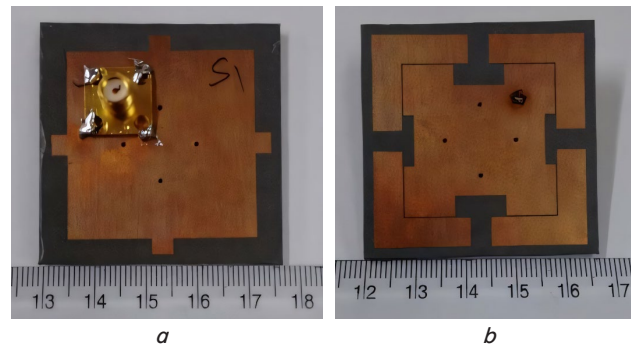

Fig. 7. Type of manufactured antenna:
a — top view; b — bottom view

The lower and higher resonating bands radiation patterns are observed at respective frequencies of 2.28 GHz. and 3.15 GHz. The responses are analyzed by using HFSS and experimental setup. The respective plots are depicted in Fig. 9, 10. The empirical and simulated gains of the antenna are depicted in Fig. 11.

The close correspondence between the simulation and experimental results for the characteristics of return loss (RLC) and axial ratio (AR) can be explained by the exact realization of vertical metal transitions and fractal Minkowski curves. These structural elements effectively control the distribution and polarization of the electromagnetic field, which leads to improved bandwidth and polarization purity at both higher and lower resonant frequencies. Compared to existing antenna designs, Ant8 demonstrates excellent dual-band performance and circular polarization. The achieved throughput values of 27.84 % and 6.11 % with return loss at various frequencies exceed the typical results described in the literature, which emphasizes the effectiveness of the proposed design.
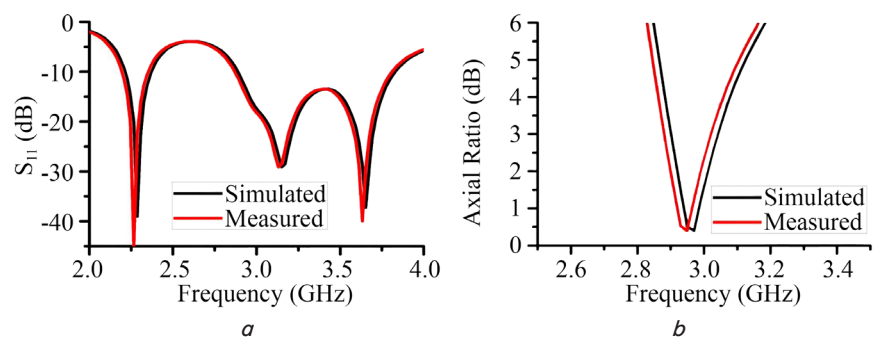

Fig. 8. Simulation and experimental results:
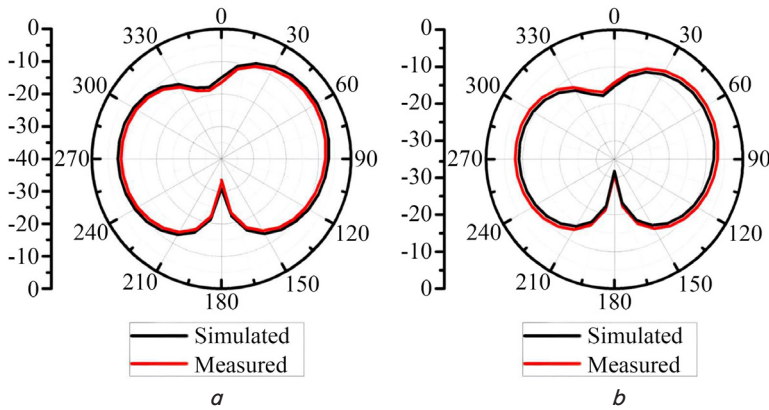a — return loss characteristics; b — axial ratio characteristics

Fig. 9. At 2.28 GHz, simulations and measurements were performed:
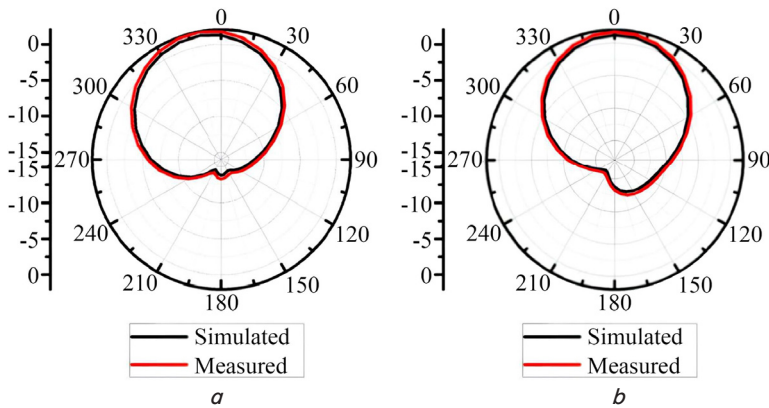a — E plane; b — H planes

Fig. 10. At 3.15 GHz, simulations and measurements were performed:
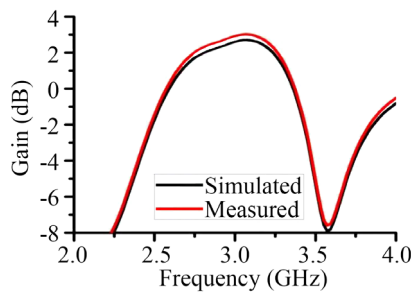a — E plane; b — H planes

Fig. 11. The proposed Ant8 gain characteristics plot

During the study, limitations were identified regarding the reproducibility of the results under various environmental conditions and input parameters. Although the antenna works well in the specified frequency ranges (2.4 GHz and 3.4 GHz), deviations may occur outside these ranges or in non-ideal testing conditions. Ensuring reliability in wider operating conditions will require further verification and optimization. A notable disadvantage is the difficulty of manufacturing antennas with precise geometric configurations and using materials such as metamaterials. In future research, this problem could be solved by studying simplified manufacturing techniques or alternative materials that have similar electromagnetic properties without the associated manufacturing difficulties. Future developments may be aimed at expanding the antenna's frequency adaptation and miniaturization capabilities. However, there may be problems in balancing miniaturization and maintaining performance metrics such as gain and radiation efficiency. Methodologically, improving

the accuracy of modeling and experimental verification of methods will be crucial to overcome these problems.

Given these considerations, future research can build on the foundation laid by Ant8, which will further expand its practical applicability and advance the field of microstrip patch antenna design for modern wireless communication systems.

6. Discussion of the results of the study of Minkowski fractal antennas

The close correspondence between the simulation and experimental results for the characteristics of return loss (RLC) and axial ratio (AR) can be explained by the precise realization of vertical metal transitions and fractal Minkowski curves. These structural elements effectively control the distribution and polarization of the electromagnetic field, leading to improved bandwidth and polarization purity at both higher and lower resonant frequencies. This is evidenced by the RLC measurements displayed in Fig. 8, a, which show a harmonious alignment between empirical and simulated data. Similarly, the AR characteristics shown in Fig. 8, b confirm the effectiveness of the design in achieving the desired polarization performance. The radiation pattern characteristics measured in the anechoic chamber, depicted in Fig. 9, 10, further validate the dual-band operation and confirm the theoretical predictions.

The Ant8 design demonstrates significant advancements over existing antenna designs, particularly in terms of dual-band performance and circular polarization. The achieved return loss bandwidths of 27.84 % (2.88–3.81 GHz) and 6.11 % (2.22–2.36 GHz) due to current at VIAs surpass typical results reported in the literature, underscoring the superiority of the proposed design. The empirical and simulated gains of the antenna, as depicted in Fig. 11, further highlight its enhanced performance metrics.

The proposed method of incorporating vertical metal transitions and fractal Minkowski curves stands out due to its ability to effectively manage electromagnetic field distribution and polarization, leading to improved performance metrics. Compared to existing works, such as the dual-band designs in [3, 8–14] and the circular polarization techniques in [5, 15–23], the Ant8 design exhibits a broader return loss bandwidth and better polarization purity. For instance, while [3] achieved significant bandwidth and isolation improvements with a trident-shaped antenna, the Ant8 design extends these improvements further by enhancing dual-band operation and achieving more robust circular polarization.

Despite the significant advancements, the study identified several limitations regarding the reproducibility of the results under various environmental conditions and input parameters. Although the antenna performs well in the specified frequency ranges (2.4 GHz and 3.4 GHz), deviations may occur outside these ranges or under non-ideal testing conditions. This indicates a need for further verification and optimization to ensure reliability in broader operating conditions. Additionally, the complex manufacturing process of antennas

with precise geometric configurations and the use of materials such as metamaterials pose significant challenges. A notable disadvantage of this study is the difficulty of manufacturing antennas with precise geometric configurations using metamaterials. This challenge could be addressed in future research by exploring simplified manufacturing techniques or alternative materials with similar electromagnetic properties.

Future research may focus on expanding the antenna's frequency adaptation and miniaturization capabilities. However, this may present challenges in balancing miniaturization while maintaining performance metrics such as gain and radiation efficiency. Methodologically, enhancing the accuracy of modeling and experimental verification methods will be critical. Potential difficulties could include mathematical challenges in optimizing the design for different frequency ranges and experimental challenges in achieving consistent manufacturing quality. Further development of the Ant8 design will build on its established foundation, advancing the field of microstrip patch antenna design for modern wireless communication systems.

The study identified several limitations regarding the reproducibility of the results under various environmental conditions and input parameters. Although the antenna performs well in the specified frequency ranges (2.4 GHz and 3.4 GHz), deviations may occur outside these ranges or under non-ideal testing conditions. This indicates a need for further verification and optimization to ensure reliability in broader operating conditions. Additionally, the complex manufacturing process of antennas with precise geometric configurations and the use of materials such as metamaterials pose significant challenges.

A notable disadvantage of this study is the difficulty of manufacturing antennas with precise geometric configurations using metamaterials. This challenge could be addressed in future research by exploring simplified manufacturing techniques or alternative materials with similar electromagnetic properties. Another area for improvement is the accuracy of modeling and experimental verification methods, which is crucial for overcoming the identified limitations.

7. Conclusions

1. The suggested patch antenna design effectively utilizes fractal Minkowski curves and strategic vertical interconnect placements to achieve dual-band performance with circular polarization at the upper frequency band and enhanced left-hand frequency response at the lower band. The integration of these advanced design elements, including the coaxial probe feed positioned diagonally and VIAs placed 7 mm from the patch center, results in a highly efficient antenna with improved bandwidth and minimal signal reflection. This innovative approach confirms the antenna's capability to meet the specified performance criteria.

2. The antenna design achieves a notable 10-dB return loss bandwidth of 6.11 % at lower resonating frequencies, highlighting its versatility in maintaining efficient signal reception and transmission across different frequency bands. This quantitative indicator underscores its suitability for diverse applications requiring reliable communication over varied frequency ranges. The achievement reflects advancements in antenna engineering, employing innovative design strategies to mitigate signal interference and ensure stable operation in diverse wireless communication environments.

3. Notably, the antenna architecture achieves a 3-dB axial ratio bandwidth of 5.05 % at the upper band, demonstrating superior circular polarization characteristics essential for minimizing signal degradation and optimizing data throughput in wireless networks. This qualitative indicator represents a significant advancement in antenna performance, surpassing traditional designs in polarization purity and signal fidelity. The enhanced axial ratio bandwidth is facilitated by optimized parasitic elements and metamaterial enhancements, enhancing the antenna's ability to maintain polarization integrity across the WiMAX band (3.4 GHz) and WLAN band (2.4 GHz).

References

1. Naga Jyothi Sree, G., Nelaturi, S. (2021). Design and experimental verification of fractal based MIMO antenna for lower sub 6-GHz 5G applications. AEU – International Journal of Electronics and Communications, 137, 153797. https://doi.org/10.1016/j.aeue.2021.153797

2. Sharma, P., Tiwari, R. N., Singh, P., Kanaujia, B. K. (2022). Dual-band trident shaped MIMO antenna with novel ground plane for 5G applications. AEU – International Journal of Electronics and Communications, 155, 154364. https://doi.org/10.1016/j.aeue.2022.154364

3. Cao, W. (2016). Compact dual-band dual-mode circular patch antenna with broadband unidirectional linearly polarised and omnidirectional circularly polarised characteristics. IET Microwaves, Antennas & Propagation, 10 (2), 223–229. https://doi.org/10.1049/iet-map.2015.0266

4. Reddy, V. V., Sarma, N. V. S. N. (2014). Compact Circularly Polarized Asymmetrical Fractal Boundary Microstrip Antenna for Wireless Applications. IEEE Antennas and Wireless Propagation Letters, 13, 118–121. https://doi.org/10.1109/lawp.2013.2296951

5. Reddy, V. V., Sarma, N. V. S. N. (2014). Triband Circularly Polarized Koch Fractal Boundary Microstrip Antenna. IEEE Antennas and Wireless Propagation Letters, 13, 1057–1060. https://doi.org/10.1109/lawp.2014.2327566

6. Hassan Ghadeer, S., Kamal Abd.Rahim, S., Alibakhshikenari, M., Virdee, B. S., Elwi, T. A., Iqbal, A., Al-Hasan, M. (2023). An innovative fractal monopole MIMO antenna for modern 5G applications. AEU - International Journal of Electronics and Communications, 159, 154480. https://doi.org/10.1016/j.aeue.2022.154480

7. Raja, K. B., Pandian, S. C. (2022). Low-profile metamaterial-based T-shaped engraved electrically small antenna design with wideband operating capability for WLAN/5G applications. Physica B: Condensed Matter, 646, 414359. https://doi.org/10.1016/j.physb.2022.414359

8. Tiwari, D., Ansari, J. A., Saroj, A. Kr., Kumar, M. (2020). Analysis of a Miniaturized Hexagonal Sierpinski Gasket fractal microstrip antenna for modern wireless communications. AEU – International Journal of Electronics and Communications, 123, 153288. https://doi.org/10.1016/j.aeue.2020.153288

9. Eleftheriades, G. V., Balmain, K. G. (Eds.) (2005). Negative-Refraction Metamaterials. John Wiley & Sons. https://doi.org/10.1002/0471744751

10. Caloz, C., Itoh, T. (2005). Electromagnetic Metamaterials: Transmission Line Theory and Microwave Applications. John Wiley & Sons. https://doi.org/10.1002/0471754323

11. Sanada, A., Kimura, M., Awai, I., Caloz, C., Itoh, T. (2004). A planar zeroth-order resonator antenna using a left-handed transmission line. 34th European Microwave Conference.

12. Sievenpiper, D., Lijun Zhang, Broas, R. F. J., Alexopolous, N. G., Yablonovitch, E. (1999). High-impedance electromagnetic surfaces with a forbidden frequency band. IEEE Transactions on Microwave Theory and Techniques, 47 (11), 2059–2074. https://doi.org/10.1109/22.798001

13. Lai, A., Caloz, C., Itoh, T. (2004). Composite right/left-handed transmission line metamaterials. IEEE Microwave Magazine, 5 (3), 34–50. https://doi.org/10.1109/mmw.2004.1337766

14. Lee, C.-J., Leong, K. M. K. H., Itoh, T. (2006). Composite Right/Left-Handed Transmission Line Based Compact Resonant Antennas for RF Module Integration. IEEE Transactions on Antennas and Propagation, 54 (8), 2283–2291. https://doi.org/10.1109/tap.2006.879199

15. Yuandan Dong, Toyao, H., Itoh, T. (2011). Compact Circularly-Polarized Patch Antenna Loaded With Metamaterial Structures. IEEE Transactions on Antennas and Propagation, 59 (11), 4329–4333. https://doi.org/10.1109/tap.2011.2164223

16. Saurav, K., Sarkar, D., Srivastava, K. V. (2014). Dual-Polarized Dual-Band Patch Antenna Loaded With Modified Mushroom Unit Cell. IEEE Antennas and Wireless Propagation Letters, 13, 1357–1360. https://doi.org/10.1109/lawp.2014.2337911

17. Park, J.-H., Ryu, Y.-H., Lee, J.-G., Lee, J.-H. (2007). Epsilon Negative Zeroth-Order Resonator Antenna. IEEE Transactions on Antennas and Propagation, 55 (12), 3710–3712. https://doi.org/10.1109/tap.2007.910505

18. Tang, H., Zhao, X. (2009). Center-fed circular Epsilon-negative zeroth-order resonator antenna. Microwave and Optical Technology Letters, 51 (10), 2423–2428. https://doi.org/10.1002/mop.24639

19. Cao, W.-Q., Zhang, B.-N., Liu, A. J., Guo, D.-S., Yu, T.-B., Wei, Y. (2012). A Dual-Band Microstrip Antenna with Omnidirectional Circularly Polarized and Unidirectional Linearly Polarized Characteristics Based on Metamaterial Structure. Journal of Electromagnetic Waves and Applications, 26 (2-3), 274–283. https://doi.org/10.1163/156939312800030811

20. Cao, W.-Q., Liu, A. J., Zhang, B.-N., Yu, T.-B., Guo, D.-S., Wei, Y., Qian, Z.-P. (2012). Multi-Band Multi-Mode Microstrip Circular Patch Antenna Loaded With Metamaterial Structures. Journal of Electromagnetic Waves and Applications, 26 (7), 923–931. https://doi.org/10.1080/09205071.2012.710377

21. Cao, W., Liu, A., Zhang, B., Yu, T., Qian, Z. (2013). Dual-Band Spiral Patch-Slot Antenna With Omnidirectional CP and Unidirectional CP Properties. IEEE Transactions on Antennas and Propagation, 61 (4), 2286–2289. https://doi.org/10.1109/tap.2012.2235400

22. Baibolov, A., Sydykov, S., Alibek, N., Tokmoldayev, A., Turdybek, B., Jurado, F., Kassym, R. (2022). Map of zoning of the territory of Kazakhstan by the average temperature of the heating period in order to select a heat pump system of heat supply: A case study. Energy Sources, Part A: Recovery, Utilization, and Environmental Effects, 44 (3), 7303–7315. https://doi.org/10.1080/15567036.2022.2108168

23. Bimurzaev, S., Aldiyarov, N., Yerzhigitov, Y., Tlenshiyeva, A., Kassym, R. (2023). Improving the resolution and sensitivity of an orthogonal time-of-flight mass spectrometer with orthogonal ion injection. Eastern-European Journal of Enterprise Technologies, 6 (5 (126)), 43–54. https://doi.org/10.15587/1729-4061.2023.290649